

INSTITUTO DE FÍSICA

preprint

IFUSP/P 284
B.I.F. - USP

IFUSP/P-284

B.I.F. - USP

LIMITING ANGULAR MOMENTA FOR LIGHT HEAVY ION FUSION AT
HIGH ENERGY

A.Szanto de Toledo, T.M.Cormier, M.Herman, B.Lin,
P.M.Stwertka, M.M.Coimbra and N.Carlin Filho

AUG/81

UNIVERSIDADE DE SÃO PAULO
INSTITUTO DE FÍSICA
Caixa Postal - 20.516
Cidade Universitária
São Paulo - BRASIL

LIMITING ANGULAR MOMENTA FOR LIGHT HEAVY ION FUSION
AT HIGH ENERGY[†]

A. Szanto de Toledo

Instituto de Física da Universidade de São Paulo - Lab. Pelletron -
Caixa Postal 20516 - São Paulo - Brasil and
Department of Physics - University of Rochester

T.M. Cormier*, M. Herman, B. Lin and P.M. Stwertka
Department of Physics - University of Rochester

and

M.M. Coimbra and N. Carlin Filho

Instituto de Física da Universidade de São Paulo - Lab. Pelletron -
Caixa Postal 20516 - São Paulo - Brasil

A B S T R A C T

The shapes of angular distributions in $^{12}\text{C}(^{16}\text{O},\alpha)$ reactions to the $J^\pi = 0^+$ ^{24}Mg -ground state are studied from $E(^{16}\text{O}) = 28.5$ MeV to 100 MeV. The position of the first minimum (and maximum) of these oscillatory angular distributions is expected to be sensitive to the presence of a low angular momentum cut off in the compound nucleus formation cross section. No evidence for a low-L cut off is found even at energies well beyond the predicted threshold.

[†] This work was supported in part by the National Science Foundation and CNPq - Brasil.

* Supported in part by the Alfred P. Sloan Foundation.

2.

Time dependent Hartree Fock Theory predicts the inhibition of low impact parameter fusion in nucleus-nucleus collisions at high energy⁽¹⁾. This fact has provoked a number of experimental investigations attempting to isolate the effect^(2,3). An unambiguous result, however, has not been forthcoming chiefly because the low partial waves make an extremely small contribution to the fusion cross section. Recently, it has been shown by Szanto de Toledo et al.⁽⁴⁾ that the presence of a low-L cut off will strongly influence the angular cross-correlation and the shapes of zero-channel-spin angular distributions in statistical compound nucleus decay. In the present letter we report the results of applying this method to the fusion of $^{16}\text{O} + ^{12}\text{C}$.

We have studied the ground state transition of the $^{12}\text{C}(^{16}\text{O},\alpha)^{24}\text{Mg}$ reaction from $E(^{16}\text{O}) = 28.5$ MeV to 100 MeV. The shapes of the α_0 angular distributions have been analyzed within the statistical model frame-work. Our results show no significant deviation from compound nucleus predictions using no low-L cut off. Upper limits for the minimum angular momentum contributing to $^{16}\text{O}+^{12}\text{C}$ fusion are established up to $E(^{16}\text{O})=100$ MeV.

Angular momentum matching conditions in statistical compound nucleus decay to a discrete state force a localization of the contributing partial cross sections, σ_J , in angular momentum space. The distribution of σ_J is strongly peaked with a center of gravity $\langle J \rangle$, the mean compound nucleus spin contributing to the excitation of the final state^(5,6). If a low angular momentum cut off occurs in the entrance channel, the average compound nucleus spin distribution is shifted to a higher value with a

corresponding increase in $\langle J \rangle$. In the case of zero channel spin reactions, the angular distributions display an oscillatory behavior with a period related to $\langle J \rangle$ and a damping factor related to the width of the σ_J distribution. Consequently the truncation of the low-L components of σ_J modify the shape and period of the angular distribution^(4,5). This effect can be investigated by following the energy dependence of the angles of the first minimum (φ) and first maximum (ϕ) of the α_0 angular distribution.

The statistical model gives approximately⁽⁵⁾ $\varphi \approx 3\pi/4 \langle J \rangle$ and $\phi = 5\pi/4 \langle J \rangle$, and for zero channel-spin, $\langle J \rangle$ is approximately the grazing angular momentum L_g^α of the outgoing particle. Thus in the absence of a low-L cutoff one expects that φL_g^α and ϕL_g^α are constant and independent of bombarding energy:

$$\varphi L_g^\alpha = \varphi \left[\frac{2\mu R^2}{\hbar^2} (E+Q) - \frac{ZZ'e^2}{R} \right]^{1/2} = 3\pi/4 \quad (1)$$

$$\text{and } \phi L_g^\alpha = 5\pi/4$$

Measurements were made on the University of Rochester MP Tandem and the University of São Paulo 8UD Pelletron. Silicon position sensitive detectors were used for $E(^{16}\text{O}) < 55$ MeV and the Rochester split pole spectrograph for > 55 MeV. An accurate angle calibration was achieved in both cases based on measurements at both positive and negative angles to determine true zero degrees.

Bombarding energy averaged α -spectra (Fig. 1A) were obtained by using either a thick self supporting C foil ($\Delta E(^{16}\text{O}) = 1.2$ to 1.8 MeV) or by explicitly averaging

the angular distributions measured in fine steps ($\Delta E(^{16}\text{O}) = 300$ KeV). This procedure should virtually eliminate Ericson fluctuations.

The excitation function for the α_0 -differential cross section at the angle θ of the first maximum is shown in fig. 1B. The dashed lines represent a Hauser-Feshbach calculation performed using the code STATIS⁽⁶⁾. Averaged level density parameters were adjusted in order to reproduce the experimental cross section at $E_{\text{LAB}} = 51$ MeV ($a \sim A/6$). An uncertainty of 25% is attributed to the absolute experimental cross section due mainly to uncertainties in target thickness determination. In this calculation, no low-L cutoff has been applied, and a L_c -critical value has been used: $L_c = (\sigma_{\text{fus}}/\pi\lambda^2)^{1/2} - 1$ where the experimental fusion cross section σ_{fus} has been taken from reference (7).

Some typical angular distributions are shown in fig. 2. The small points are least square fits to sums of Legendre polynomials $\left[\frac{d\sigma}{d\Omega} = \sum a_k P_k(\cos\theta) \right]$ used to extract precisely the values of φ and ϕ from the experimental data.

The full lines represent statistical model calculations. An absolute renormalization smaller than 25% has been allowed (see fig. 1B). No low-L-cutoff has been applied in these calculations.

The energy dependence of φ and ϕ plotted times L_g^α , from eq. 1, is shown in fig. 3. The vertical error bars give the angle uncertainty resulting from counting statistics

and fitting, and the horizontal error bar gives the energy averaging interval. The solid line gives the prediction of a full Hauser-Feshbach statistical model calculation (STATIS⁽⁶⁾) assuming no low-L cutoff while the dashed line shows the effect of including a low-L cutoff given by

$$L_{\min}^2 = \frac{2.4R^2}{h^2} \left\{ E_{\text{CM}} - \frac{ZZ'e^2}{R} - \frac{A_2(A_1+A_2)}{A_1} \left(\left(1 + \frac{B}{\epsilon_F}\right)^{1/2} - 1 \right) \epsilon_F \right\} \quad (2)$$

where $\epsilon_F = 35$ MeV, $B = 8$ MeV and $A_2 > A_1$ and $R = 1.4(A_1^{1/3} + A_2^{1/3})$. This equation has been shown⁽¹⁾ to contain the essential ingredients of the time dependent Hartree-Fock theory and in particular is in accord with full TDHF calculations for $^{16}\text{O} + ^{16}\text{O}$ ⁽¹⁾ and, $^{12}\text{C} + ^{12}\text{C}$ ⁽¹⁾ and $^{16}\text{O} + ^{27}\text{Al}$ ⁽⁸⁾.

Since a sharp cutoff approximation is used in the calculations and only integer L values are used, the theoretical trajectory in the $\psi_{L_g}^{\alpha} \times E_L$ plane (dashed lines) has been smoothed.

Figure 3 shows clearly that no significant deviation from the $L_{\min} = 0$ statistical model calculation is observed. To illustrate the effect of the inclusion of a low-L cut off on the shape of the angular distribution, the 100 MeV plot in fig. 2, shows also the theoretical prediction (dashed line) when the predicted value of L_{\min} is considered. A drastic change in the oscillatory behaviour is then observed.

To eliminate the influence of the parameters of the statistical model calculations, on the results, the energy dependence of the transmission coefficient has been investigated in order to fit the low energy data, ($E_L < 55$ MeV), below the L_{\min} threshold. All the parameters used in the statistical model calculations, with the exception of the limiting angular momenta values, have been kept fixed.

To estimate limits for L_{\min} values, as a function of the bombarding energy, χ^2 fits to the shape of the predicted angular distributions (as a function of L_{\min}) have been performed (fig. 4).

The decrease of the χ^2 , even at low- L_{\min} values indicates that these low angular momentum partial waves still contribute to the compound nucleus formation, even at energies well beyond the predicted threshold. For very low L-values, our method becomes insensitive due to the localization, in the angular momentum space, of the contributing compound nucleus partial cross sections (σ_J) to the ground state transition.

In conclusion, the experimental angular distributions of the $^{12}\text{C}(^{16}\text{O}, \alpha_0)$ transition were measured in a wide energy interval $28.5 \text{ MeV} \leq E_L \leq 100 \text{ MeV}$, and are reproduced by statistical model calculations without the need of a low-L-cutoff in the σ_J -distributions of the compound nucleus angular momenta. Results of the present work suggest upper limits for L_{\min} that are much lower than the values predicted by the Time Dependent Hartree-Fock theory. However, a probing to even lower L-components could be performed investigating the evaporation of lighter particles, i.e., protons and neutrons in spite of the experimental difficulties which may arise from the lack of selectivity.

One of us (AST) acknowledge the kind hospitality at the Nuclear Structure Research Laboratory - Rochester.

REFERENCES

1. P. Bonche, S.E. Koonin and J.W. Negele, Phys. Rev. C13, 1226 (1976).
S.E. Koonin, K.T.R. Davies, V. Maruhn-Regwani, H. Feldmeir, S.J. Drieger and J.W. Negele, Phys. Rev. C15, 1359 (1977).
Cheuk-Yin-Wong, in Proceedings of the Time-Dependent-Hartree-Fock Workshop, Paris, France, 28 May - 1 June, 1979 (to be published).
2. S. Kox, A.J. Cole and R. Ost, Phys. Rev. Lett. 44, 1204 (1980).
3. B. Natowitz, G. Doukellis, B. Kolb, G. Rosner and Th. Walcher, Nucleonika 24, 443 (1979).
A. Lazzarini, H. Doubre, K.T. Lesko, V. Metag, A. Seamster, R. Vandenbosh and W. Merryfield, Phys. Rev. C24, 309 (1981).
4. A. Szanto de Toledo and M.S. Hussein, Phys. Rev. Lett. 46, 985 (1981).
5. M.S. Hussein and A. Szanto de Toledo - Preprint IFUSP/P-265 and to be published.
6. R.G. Stokstad, Wright Nuclear Structure Laboratory, Yale University, Internal Report No. 52, 1972 (unpublished).
7. Kovar et al., Phys. Rev. C20, 2147 (1979) and references therein.
8. K.R.S. Devi, A.K. Dhar and M.R. Strayer, Phys. Rev. C23, 2062 (1981).
9. When $L_{\min} \neq 0$ values are considered in the calculations, the maximum angular momentum L_{\max} allowed for the compound nucleus is recalculated such that the experimental fusion cross section is reproduced, i.e.,

$$(L_{\max} + 1)^2 - (L_{\min} + 1)^2 = \frac{\sigma_{\text{fus}}}{\pi k^2}$$

FIGURE CAPTIONS

FIGURE 1:

- 1A: Typical α -spectra observed at $E_{\text{LAB}} = 55$ MeV and 100 MeV.
- 1B: Excitation function of the ground state transition: $(\frac{d\sigma}{d\Omega})$ at the first maximum angle ϕ . The dashed line shows the theoretical prediction assuming $J_{\min} = 0$.

FIGURE 2:

Typical angular distributions. The small points correspond to least square fits to sums of Legendre Polynomial. The full lines show the result of statistical model calculations assuming $J_{\min} = 0$. The dashed line at $E_{\text{LAB}} = 100$ MeV is the result of the same calculation, in which a cut off at $J_{\min} = 14 \hbar$ is applied.

FIGURE 3:

Experimental values obtained for $\phi L_g^\alpha(E_{\text{LAB}})$ and $\phi L_g^\alpha(E_{\text{LAB}})$. The full line describes the theoretical trajectory if $J_{\min} = 0$ is assumed. If the predicted J_{\min} values are considered in the calculations, the dashed trajectory is obtained.

FIGURE 4:

χ^2 fits of the shape of the experimental angular distributions to the theoretical angular distribution as a function of the low angular momentum cut off.

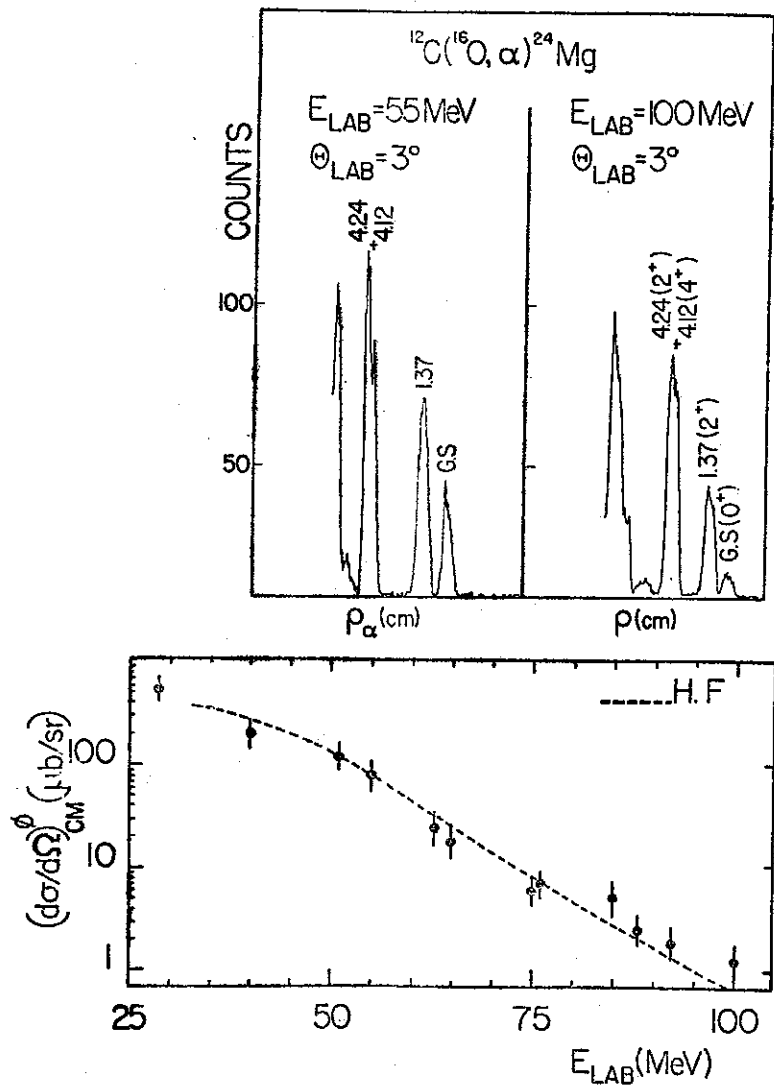


FIGURE 1

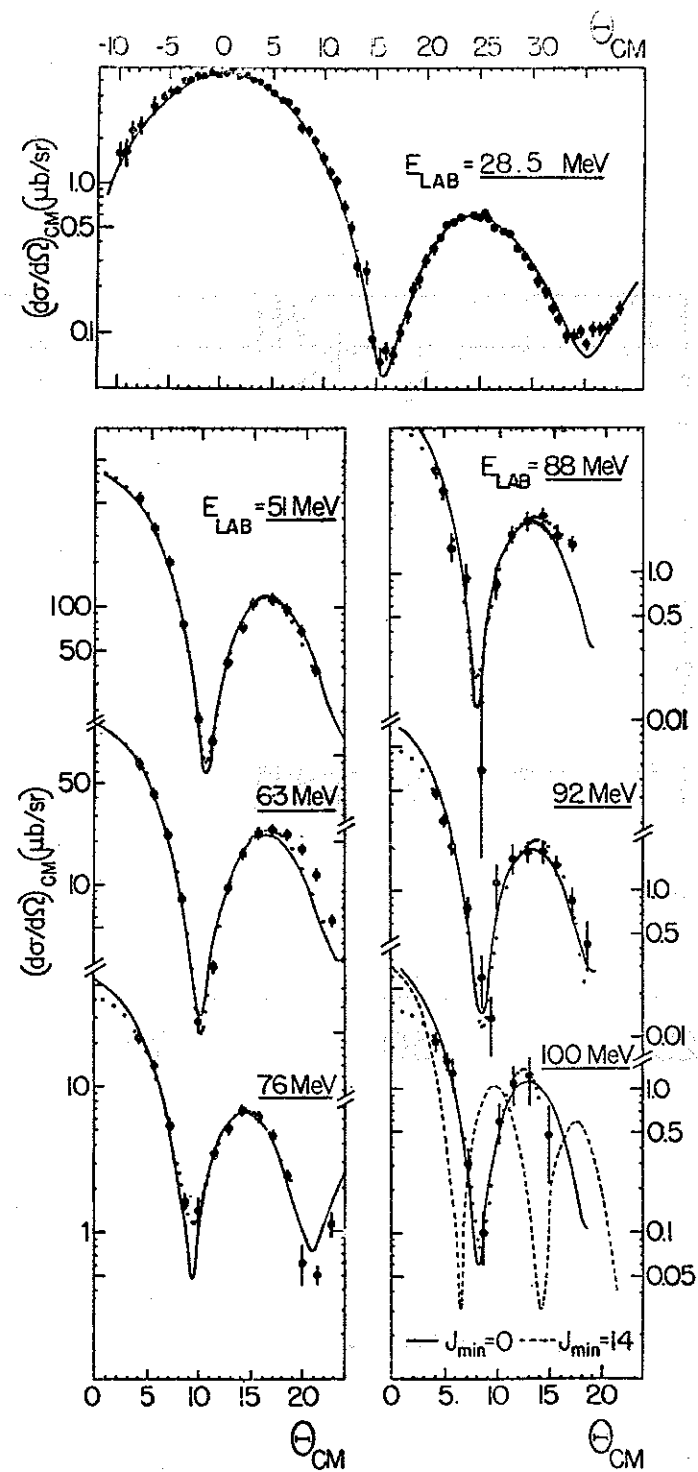


FIGURE 2

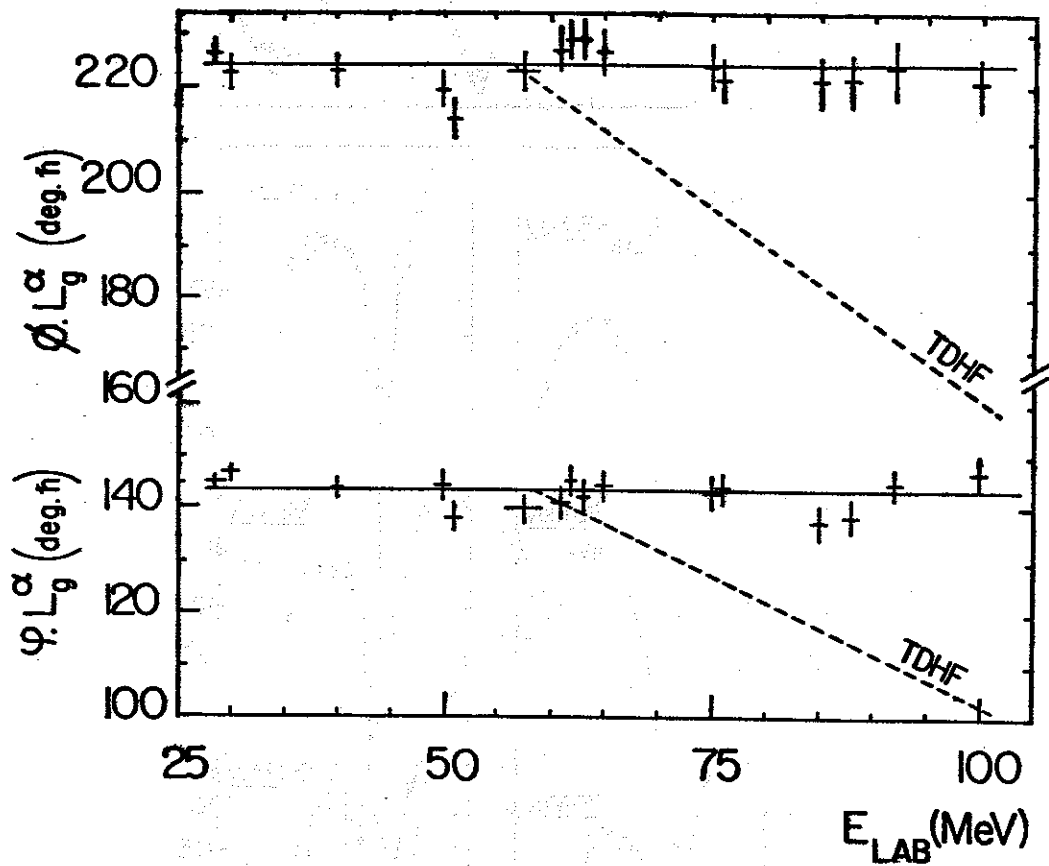


FIGURE 3

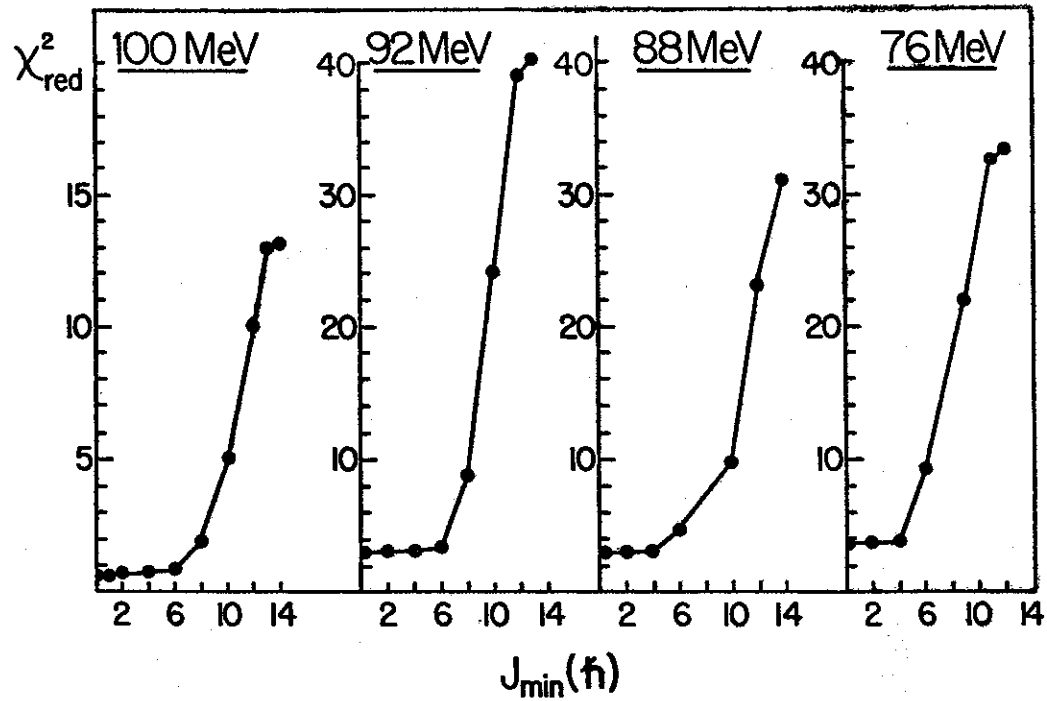


FIGURE 4